SUPPORTING INFORMATION

High Spatial Resolution MALDI Imaging Mass Spectrometry of Fresh-Frozen Bone

Christopher J. Good,[1,2] Elizabeth K. Neumann,[1,3] Casey E. Butrico,[4] James E. Cassat,[4,5,6,7] Richard M. Caprioli,[1,2,3,8,9] and Jeffrey M. Spraggins[1,2,3,10] *

[1]Mass Spectrometry Research Center, Vanderbilt University, Nashville, TN 37235, USA;
[2]Department of Chemistry, Vanderbilt University, Nashville, TN 37235, USA;
[3]Department of Biochemistry, Vanderbilt University, Nashville, TN 37235, USA;
[4]Department of Pathology, Microbiology, and Immunology, Vanderbilt University Medical Center, Nashville, TN 37232, USA;
[5]Department of Pediatrics, Vanderbilt University Medical Center, Nashville, TN 37232, USA;
[6]Department of Biomedical Engineering, Vanderbilt University, Nashville, TN 37235, USA;
[7]Vanderbilt Institute for Infection, Immunology, and Inflammation, Vanderbilt University Medical Center, Nashville, TN 37232, USA;
[8]Department of Medicine, Vanderbilt University, Nashville, TN 37235, USA;
[9]Department of Pharmacology, Vanderbilt University, Nashville, TN 37235, USA;
[10]Department of Cell and Developmental Biology, Vanderbilt University, Nashville, TN 37235, USA

*Corresponding Author: Jeffrey M. Spraggins, jeff.spraggins@vanderbilt.edu

CONTENTS

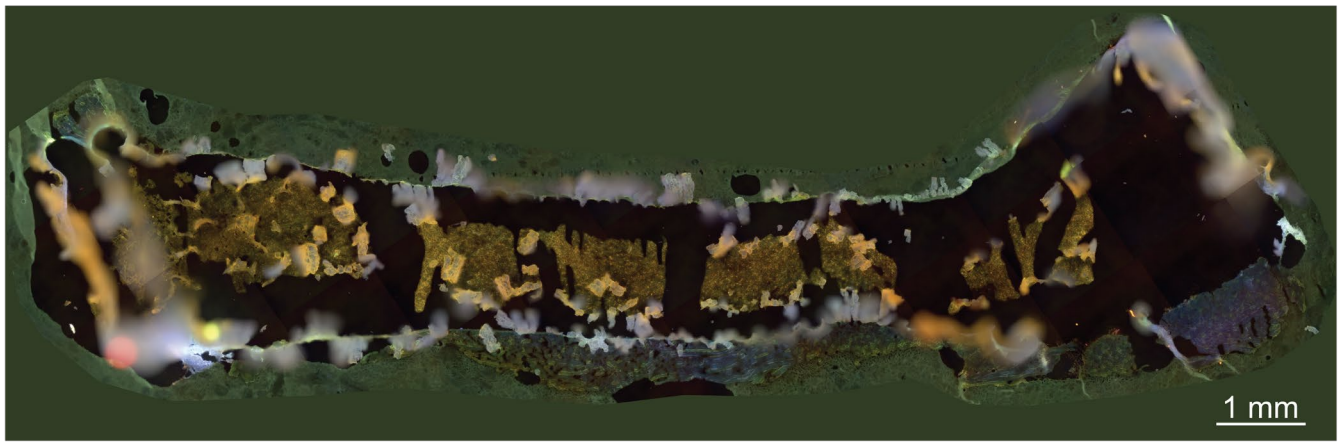

Figure S1. Cryosectioning a femur without Cryofilm leads to a notable collapse in tissue structure, as seen by the merged channel autofluorescence image.

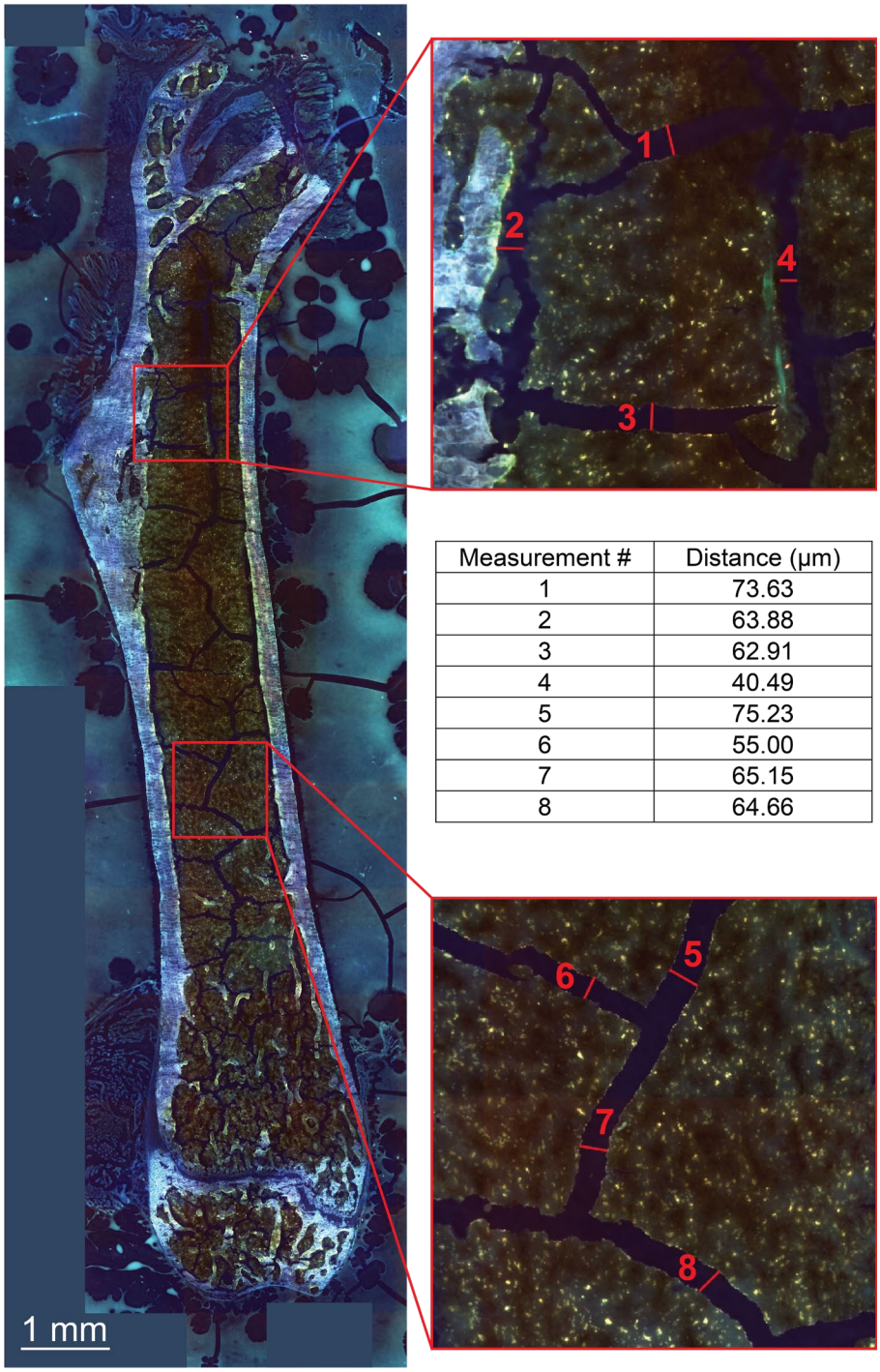

Measurement #	Distance (μm)
1	73.63
2	63.88
3	62.91
4	40.49
5	75.23
6	55.00
7	65.15
8	64.66

Figure S2. Thaw-mounting a femur section onto Cryofilm yields bone marrow cracks as large as 75 μm wide. Multiple measurements from an autofluorescence image are reported.

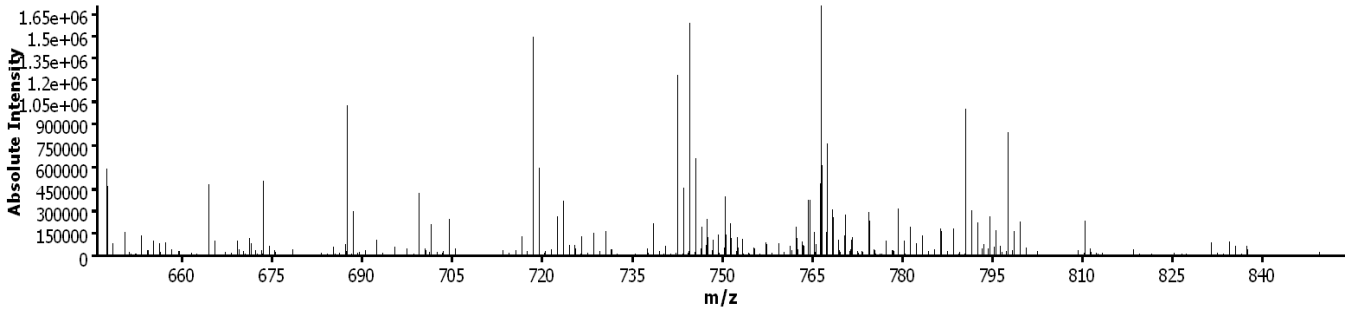

Figure S3. Sample preparation methods are compatible with negative ion mode. An unnormalized mean spectrum was acquired using the 15T Bruker solariX FT-ICR in negative ion mode. A femur section was freeze-dried and DAN was sublimed and recrystallized to yield ample lipid signal.

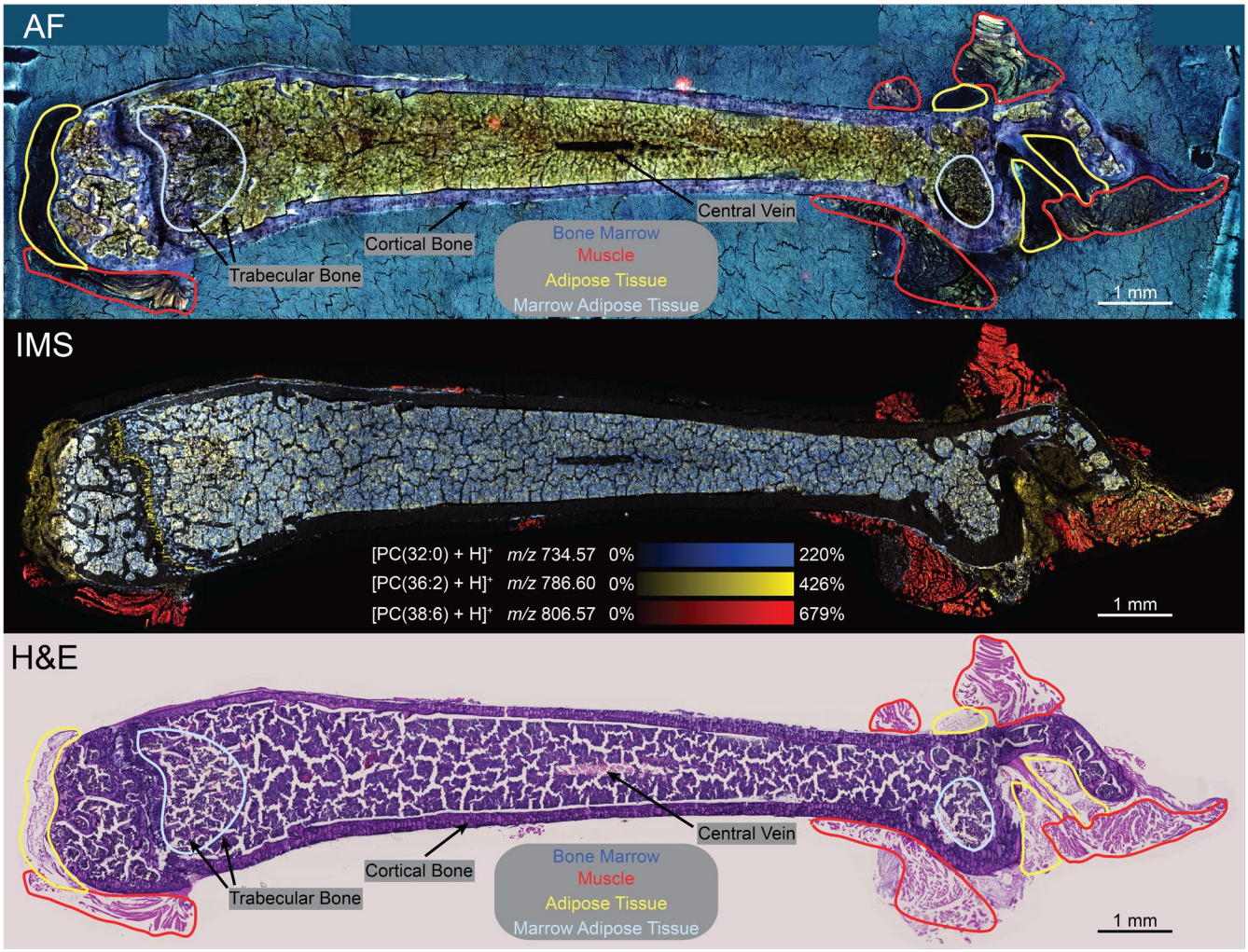

Figure S4. Sample preparation methods enable imaging of a femur section at 10 μm spatial resolution. Bone marrow artifacts are accentuated in these ion images compared to 20 μm spatial resolution ion images. Similar to Figure 5, $[PC(32:0) + H]^+$ (*m/z* 734.57), $[PC(36:2) + H]^+$ (*m/z* 786.60), and $[PC(38:6) + H]^+$ (*m/z* 806.57) localize to bone marrow, adipose tissue, and muscle, respectively. Merged channel autofluorescence (pre-IMS) and H&E stain (post-IMS) images aid in histological annotations. Ion images were not normalized.

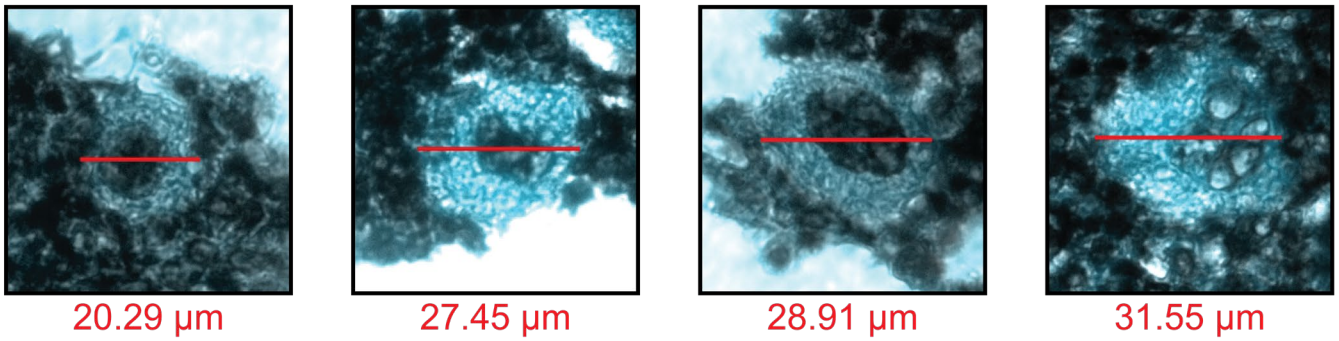

Figure S5. Megakaryocytes differ in cell diameter and nuclear configuration, which indicates variations in maturity. Images were acquired on an Axio Observer.Z1 microscope (Carl Zeiss Microscopy GmbH, Oberkochen, Germany) using a brightfield and DAPI channel.

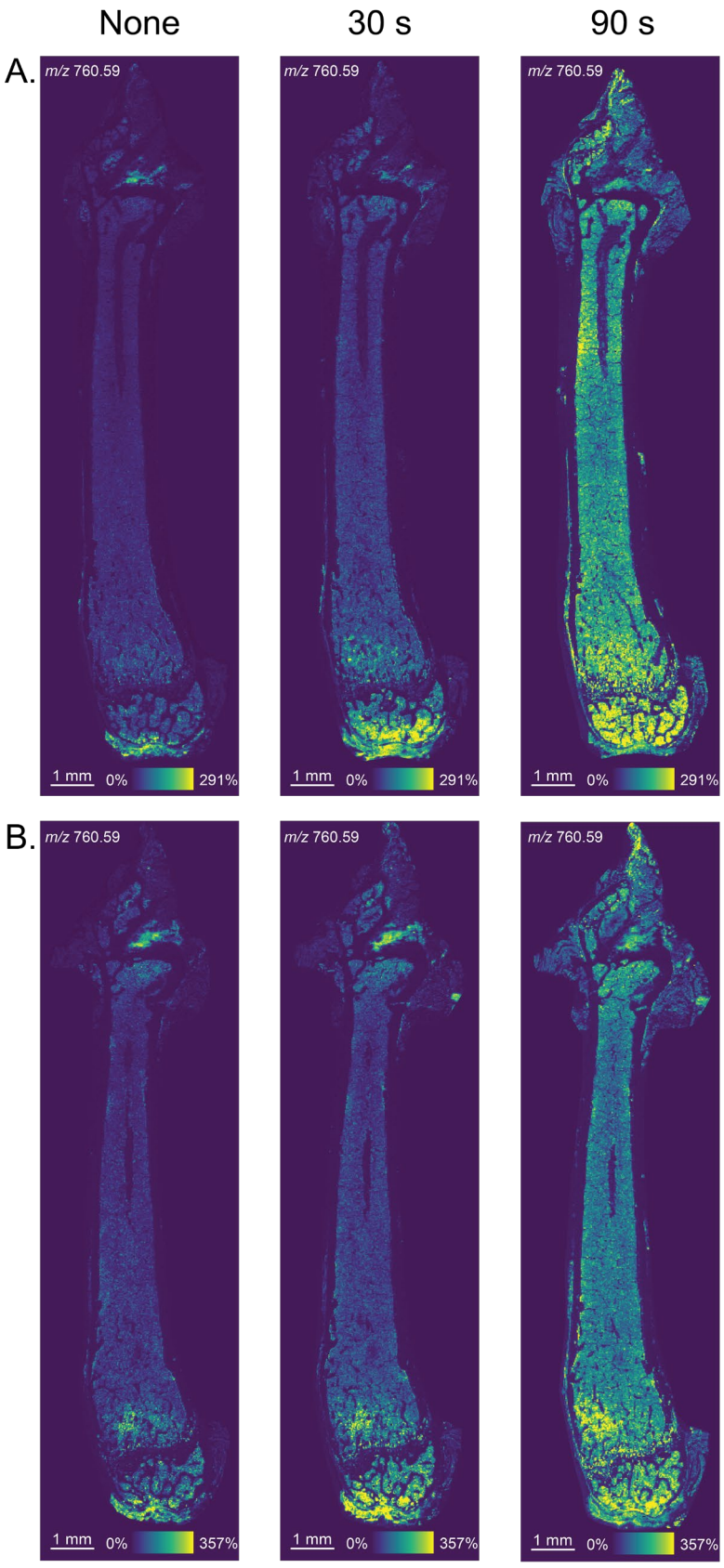

Figure S6. Unnormalized ion images highlight a reproducible intensity increase that is dependent on the duration of matrix recrystallization. (A) Ion images from Figure 3 are enlarged. (B) Ion images are from a replicate experiment.

Table S1. Additional MS parameters are reported for the Bruker timsTOF flex.

Transfer	
MALDI Plate Offset	30.0 V
Deflection 1 Delta	70.0 V
Funnel 1 RF	450.0 Vpp
isCID Energy	0.0 eV
Funnel 2 RF	500.0 Vpp
Multipole RF	500.0 Vpp
Collision Cell	
Collision Energy	10.0 eV
Collison RF	2900.0 Vpp
Quadrupole	
Ion Energy	5.0 eV
Low Mass	*m/z* 300.00
Focus Pre TOF	
Transfer Time	110.0 µs
Pre Pulse Storage	10.0 µs

Table S2. Additional MS parameters are reported for the 15T Bruker solariX FT-ICR.

Source Optics		**Octopole**	
Capillary Exit	220.0 V	Frequency	5 MHz
Detector Plate	200.0 V	RF Amplitude	350.0 Vpp
Funnel 1	150.0 V	**Quadrupole**	
Skimmer 1	60.0 V	Q1 Mass	*m/z* 610.00
Funnel RF Amplitude	250.0 Vpp	**Collision Cell**	
Transfer Optics		Collision Voltage	-1.0 V
Time of Flight	0.850 ms	DC Extract Bias	0.1 V
Frequency	4 MHz	RF Frequency	2 MHz
RF Amplitude	380.0 Vpp	Collision RF Amplitude	1200.0 Vpp
Para Cell		**In Source Fragmentation**	
Transfer Exit Lens	-20.0 V	FSCID Collision Energy	45.0 V
Analyzer Entrance	-10.0 V	**Shimming DC Bias**	
Side Kick	2.0 V	0°, 90°, 180°, 270°	1.500 V
Side Kick Offset	-1.5 V	**Gated Injection DC Bias**	
Front Trap Plate	1.500 V	0°, 90°, 180°, 270°	1.500 V
Back Trap Plate	1.500 V	**MALDI Control**	
Back Trap Plate Quench	-30.0 V	Plate Offset	100.0 V
Sweep Excitation Power	18.0 %	Deflector Plate	200.0 V

Table S3. All lipids were identified with a <1 ppm mass error tolerance. Identifications for the most intense lipid species were made using LIPIDMAPS database (lipidmaps.org).

m/z	*m/z* (database)	ID (database)	Ion	Mass Error (ppm)
703.574285	703.5748	SM 34:1; O2	$[M+H]^+$	0.732
731.605766	731.6061	SM 36:1; O2	$[M+H]^+$	0.457
734.569636	734.5694	PC 32:0	$[M+H]^+$	0.321
760.584390	760.5851	PC 34:1	$[M+H]^+$	0.933
786.600759	786.6007	PC 36:2	$[M+H]^+$	0.075
787.668742	787.6687	SM 40:1; O2	$[M+H]^+$	0.053
806.568812	806.5694	PC 38:6	$[M+H]^+$	0.729
810.600437	810.6007	PC 38:4	$[M+H]^+$	0.324
813.684935	813.6844	SM 42:2; O2	$[M+H]^+$	0.658
815.699620	815.7000	SM 42:1; O2	$[M+H]^+$	0.466

Table S4. Cryofilm-bound tissue mounted to an ITO coated glass slide consistently improves the signal intensity of PCs and SMs. Mean intensity values (arbitrary) and intensity increase percentages are reported for multiple experiments. Replicate (Rep) #1 is represented in Figure 4. An ITO coating yields an intensity increase for all replicates, but the magnitude of improvement depends on the strength of the signal.

Rep # - Slide	[PC(32:0) + H]$^+$	[PC(34:1) + H]$^+$	[PC(36:2) + H]$^+$	[PC(38:4) + H]$^+$	[SM(34:1) + H]$^+$	[SM(42:2) + H]$^+$
1 - Glass	2116.21	1731.74	645.59	325.577	451.695	110.221
1 - ITO	3540.76	2938.13	1184.14	772.337	591.31	148.671
% Increase	**67.32**	**69.66**	**83.42**	**137.22**	**30.91**	**34.88**
2 - Glass	2239	1551.72	506.618	246.92	222.719	103.957
2 - ITO	4375.88	3315.24	1106.55	689.332	624.475	188.12
% Increase	**95.44**	**113.65**	**118.42**	**179.17**	**180.39**	**80.96**
3 - Glass	539.924	101.741	33.3875	20.264	55.8127	6.7495
3 - ITO	2375.72	386.127	160.549	132.174	389.533	50.8522
% Increase	**340.01**	**279.52**	**380.87**	**552.26**	**597.93**	**653.42**